Electrical and structural properties of poly-SiGe film formed by pulsed-laser annealing

H. Watakabe and T. Sameshima[a)]
Tokyo University of Agriculture and Technology, Tokyo 184-8588, Japan

H. Kanno, T. Sadoh, and M. Miyao
Kyushu University, Hukuoka 812-8581, Japan

Electrical and structural properties of polycrystalline silicon germanium (poly-SiGe) films fabricated by pulsed-laser annealing were investigated. Observation of laser-induced melt-regrowth of SiGe films using transient conductance measurement revealed that the melt depth and the crystallization velocity increased as Ge concentration increased. The increase of the crystallization velocity resulted in increase of the average size of crystalline grains from 66 to 120 nm at the laser energy density of 360 mJ/cm^2 with increasing Ge concentration from 0 to 60%. The crystalline volume ratio obtained by reflectivity spectra in the ultraviolet region also increased from 0.83 to 1.0. Numerical analysis revealed that the density of electrically active defects decreased from 3.5×10^{18} to 1.1×10^{18} cm^{-3} as Ge concentration increased from 0 to 80%. The density of defect states of $Si_{0.8}Ge_{0.2}$ films were reduced from 3.5×10^{18} to 1.9×10^{18} cm^{-3} by 13.56-MHz hydrogen plasma treatment at 250 °C, 30 W, and 130 Pa for 30 s. However, the plasma treatment did not reduce the defect density for $Si_{0.4}Ge_{0.6}$ and $Si_{0.2}Ge_{0.8}$ films. © *2004 American Institute of Physics.* [DOI: 10.1063/1.1707216]

I. INTRODUCTION

Pulsed-laser crystallization is an attractive method with reduction of processing temperature because of local and rapid heating. It has been widely applied to formation of polycrystalline silicon (poly-Si) thin films on glass substrates for fabricating thin-film transistors (TFTs) at low processing temperatures.[1–5] Silicon germanium (SiGe) is also an attractive electronic materials in order to look for TFTs with a high hole mobility. Pulsed-laser crystallization of SiGe films, however, has not been investigated enough to apply the method to TFT fabrication. Dynamical properties of laser crystallization of SiGe films and electronic properties of poly-SiGe should be clear.

In this article, we report the analysis of electrical and structural properties of poly-SiGe films fabricated using pulsed-laser annealing. We first discuss melt-regrowth properties of SiGe films using *in situ* measurement of electrical conductivity of the films during and after laser irradiation.[6] We then show that the average grain size increases as the Ge concentration increases. We report the poly-SiGe films with a high Ge concentration have a higher crystalline volume ratio than that of poly-Si films. Analysis of defect states in the poly-SiGe films using a numerical simulation program is also reported. Moreover, we also discuss effect of hydrogen plasma treatment for the defect reduction of poly-SiGe films.

II. EXPERIMENT

Amorphous silicon germanium (a-SiGe) films, 50 nm thick, with Ge concentration from 0 (a-Si) to 80% were formed on quartz glass substrate using molecular-beam epi-

taxy equipment at room temperature.[7] They were also fabricated by plasma-enhanced chemical vapor deposition at 300 °C, 0.3 Torr using SiH_4 and GeH_4 mixture gases. Boron atoms were implanted with a concentration of 3.2×10^{18} cm^{-3} by the ion doping method with an acceleration energy at 10 keV. The a-SiGe films were crystallized using 28-ns (full width at half-maximum) XeCl excimer laser irradiation in vacuum at 1×10^{-6} Torr with no substrate heating. Five-shot multiple step laser irradiation was carried out. The laser energy density increased stepwise from 150 to 360 mJ/cm^2 with a step of 30 mJ/cm^2 for samples with Ge concentrations from 0 to 60%. For the 80% of Ge concentration samples, the maximum laser energy density was 240 mJ/cm^2 because the high Ge concentration films had lower crystallization and amorphization threshold energies.[8]

In order to investigate properties of melting and solidification of SiGe films during and after laser irradiation, the transient conductance of the films were measured. The high electrical conductivity of liquid SiGe or Si($>10^4$ S/cm) gives the melting volume and the melting duration for the films. Aluminum-gap electrodes with a width and a length of 2000 and 400 μm, respectively, were formed on undoped SiGe or Si films by vacuum evaporation and etching. A voltage was applied to the samples. The transient current during and after laser irradiation was coincidently measured as a voltage at the load resistance connected between sample and ground using a 1-GHz high-speed digital oscilloscope, as shown in Fig. 1. The electrical conductivity (σ_{SiGe}) was estimated by the equation

$$\sigma_{SiGe} = \frac{V_{out}}{\frac{W}{L} t (V_{dc} - V_{out}) R_{load}}, \tag{1}$$

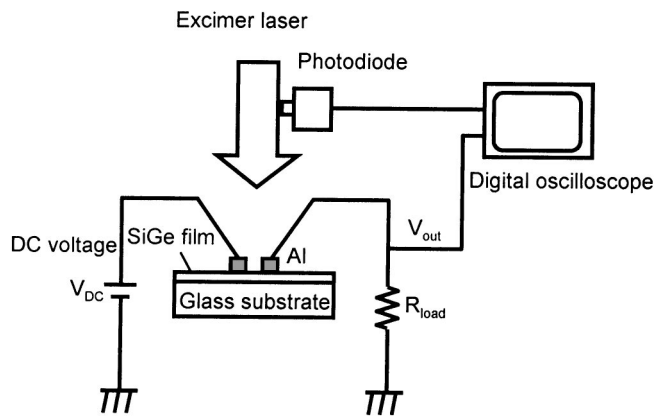a)Electronic mail: tsamesim@cc.tuat.ac.jp

6457

FIG. 1. Schematic apparatus of transient conductance measurement. The dc voltage was applied to the samples. The transient current was measured by 1-GHz high-speed digital oscilloscope.

where W and L are width and length of aluminum electrode, respectively, t is the thickness of the films, V_{dc} is the voltage applied to the samples, V_{out} is the voltage at load resistance, and R_{load} is the load resistance connected between sample and ground.

In order to observe crystalline grains of poly-SiGe films, transmission electron microscope (TEM) measurement was carried out. The crystalline volume ratio (C) was estimated by analysis of the E_2 peak, which appeared around 275 nm in optical reflectivity spectra, using a numerical calculation program constructed with the Fresnel coefficient method. The effective complex refractive index of the poly-SiGe films ($\tilde{n}_p$) is given by

$$\tilde{n}_p = C\tilde{n}_c + (1-C)\tilde{n}_a, \tag{2}$$

where $\tilde{n}_c$ and $\tilde{n}_a$ are the complex refractive indexes of single-crystalline and amorphous SiGe, respectively.[9–12] Fitting the calculated reflectivity spectra to experimental ones gave the crystalline volume ratio. In order to analyze defect states in the poly-SiGe films, $I-V$ characteristics were measured for the poly-SiGe films with different temperatures. Samples were also treated with 13.56-MHz rf hydrogen plasma treatment at 30 W, 130 Pa, and at 250 °C for 30 s.

III. RESULTS AND DISCUSSION

Melt-regrowth properties were obtained with different Ge concentrations with experimental change in the electrical conductivity, as shown by the inset in Fig. 2. The shape of change in the conductivity had two peaks because our laser pulse had two peaks of the power intensity; the first one had a high intensity and second one had a low intensity. We determined the upper limit of the electrical conductivity of solid films as 50 S/cm, which was the maximum conductivity just below the crystallization threshold. Figure 2 shows the maximum electrical conductivity of molten silicon obtained by subtracting 50 S/cm from (a) the experimental maximum electrical conductivity and (b) the melt duration as a function of Ge concentration for laser energy densities of 240 and 360 mJ/cm². The melt duration was determined as the duration for the electrical conductivity above 50 S/cm. The maximum electrical conductivity increased markedly
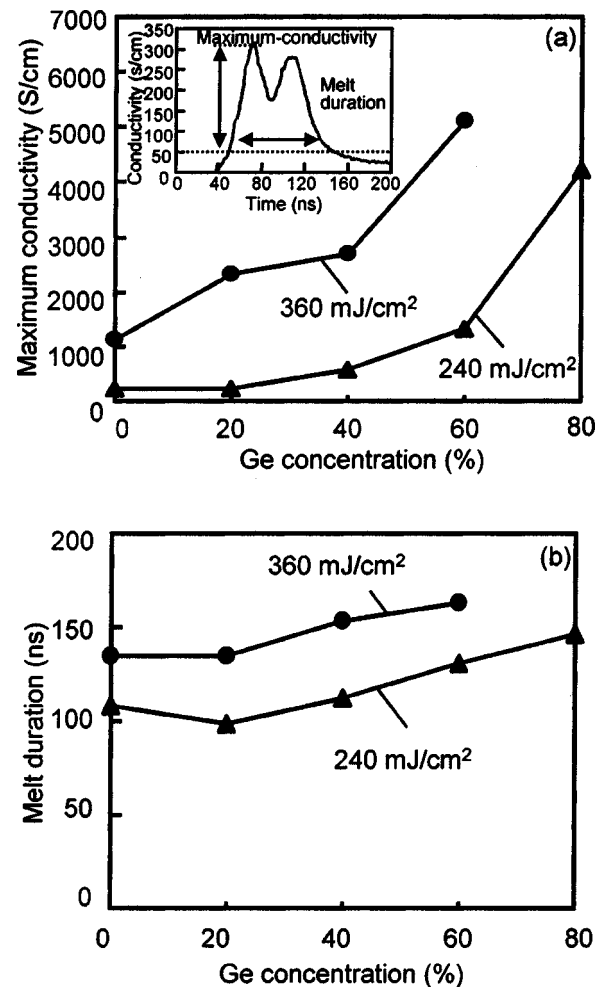

FIG. 2. Maximum electrical conductivity of molten silicon obtained by subtracting the upper limit of the electrical conductivity of solid films at 50 S/cm from (a) the experimental maximum conductivity and (b) the melt duration, which was defined as the duration for the electrical conductivity above 50 S/cm, as a function of Ge concentration for laser energy density of 240 and 360 mJ/cm². Inset shows changes in the electrical conductivity for a Ge concentration of 20% at laser irradiation of 240 mJ/cm². Dashed line shows the upper limit of solid phase conductivity.

from 210 to 4200 S/cm at 240 mJ/cm² as Ge concentration increased from 0 (poly-Si) to 80%. It also increased from 1100 to 5100 S/cm at 360 mJ/cm² as Ge concentration increased from 0 to 60%. The high maximum electrical conductivity indicates that the films with the high Ge concentration were melted deep below the surface by laser irradiation. On the other hand, the melt duration increased 30% at most as the Ge concentration increased from 0 to 80% for a laser energy of 240 mJ/cm².

The increase of the melt duration with increasing Ge concentration results from the decrease of the melting point with increasing Ge concentration. If the melt-regrowth was governed by the interface control growth, in which the interface between liquid and solid propagated in the depth direction at first (melting phase) and then came back to the surface (solidification phase), the liquid/solid interface moved quickly for films with high Ge concentration from the results shown in Fig. 2.[6,13] This means that the solidification velocity increased as the Ge concentration increased. The increase
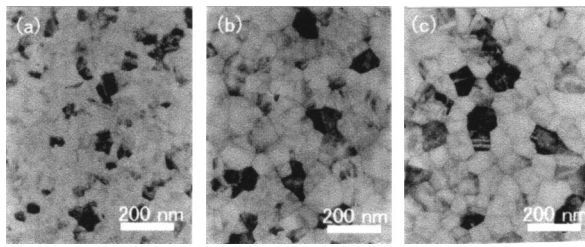
FIG. 3. Bright-field TEM images for poly-SiGe films with Ge concentrations of 20% (a), 60% (b), and 80% (c).
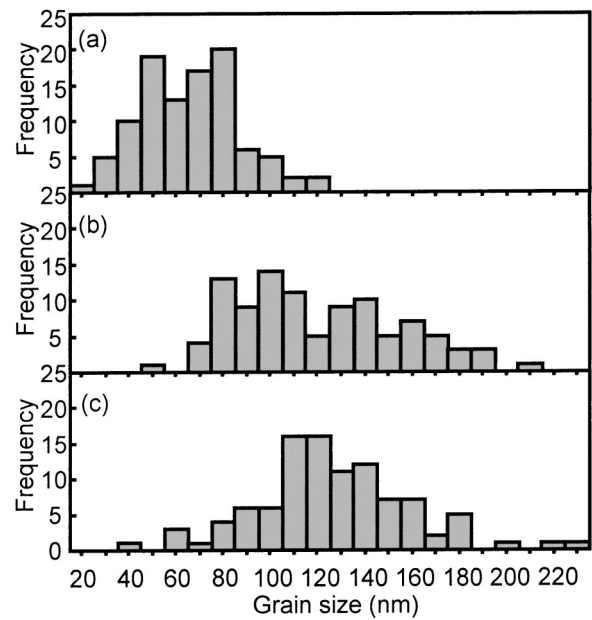

FIG. 4. Frequency of grain as a function of size for poly-SiGe films with Ge concentrations of 20% (a), 60% (b), and 80% (c) obtained by Fig. 3. One hundred crystalline grains were randomly selected and diagnosed for each Ge concentration.

of the solidification velocity probably results from the decrease of the latent heat energy at melting with increasing Ge concentration. When the latent heat energy is large, as is the case for pure silicon (1790 J/g),[14] the additional high energy is needed in order to change the solid phase to the liquid phase at the melting point. This makes the melt depth low. On the other hand, the high latent heat energy is released from the liquid phase at solidification. The liquid/solid interface is heated again by releasing latent heat energy. The increase of temperature at the interface reduces the solidification rate. On the other hand, as germanium has a low latent heat energy of 510 J/g,[14] the solid Ge can be easily changed to liquid phase at the melting point and it is melted into deep regions compared with silicon melting. In the solidification phase, the low latent heat energy does not heat Ge-liquid/solid interface so much compared with the Si melting case. The films with high Ge concentration can therefore have a high solidification velocity.

Figure 3 shows bright-field TEM images for poly-SiGe films with Ge concentration of 20% (a) 60% (b), and 80% (c). Each film was completely crystallized by laser irradiation. Crystalline grains were formed close to each other. The average size of crystalline grains obviously increased as the Ge concentration increased. Figure 4 shows the frequency of grain as a function of size for poly-SiGe films with Ge concentration of 20% (a), 60% (b), and 80% (c), obtained from Fig. 3. The grain size was defined by the longest length of every crystalline grain. The average grain size was increased from 66 to 120 nm as Ge concentration increased from 20% to 60%. Our experimental results of transient conductance shown in Fig. 2 indicate that $Si_{0.4}Ge_{0.6}$ films were melted by laser irradiation at 360 mJ/cm^2 2.2 times deeper and 1.2 times longer than $Si_{0.8}Ge_{0.2}$ films. Therefore, the solidification velocity for $Si_{0.4}Ge_{0.6}$ films was approximately 1.8 times higher than that of $Si_{0.8}Ge_{0.2}$ films. We therefore interpret that the increase of the crystalline grains with increasing Ge concentration shown in Figs. 3 and 4 results mainly from the increase of the solidification velocity. In the case of $Si_{0.2}Ge_{0.8}$ films, the average grain size was 126 nm, although the laser energy density was 240 mJ/cm^2. The crystallization of $Si_{0.2}Ge_{0.8}$ films at 240 mJ/cm^2 had the melt depth and melt duration similar to those for $Si_{0.4}Ge_{0.6}$ at 360 mJ/cm^2 (see Fig. 2). This confirms that $Si_{0.2}Ge_{0.8}$ films were crystallized with the grain size similar to that for $Si_{0.4}Ge_{0.6}$ 360 mJ/cm^2.

Figure 5 shows the crystalline volume ratio of poly-SiGe films as a function of the laser energy density for different Ge concentrations. The crystalline volume ratio increased as the laser energy density increased for each Ge concentration case. Moreover, the crystalline volume ratio increased as Ge concentration increased. In the case of poly-Si films, the crystalline volume ratio was 0.83 at laser energy density of 360 mJ/cm^2. This means that only the 83% region had an electrical band structure of crystalline silicon; the residual 17% region had a band structure associated with disordered bonding states. The crystalline volume ratio increased to 1.0 as Ge concentration increased to 60% within the resolution of the analysis ~0.03. An important reason of the high crystalline volume ratio close to 1.0 was the increase in the grain size as shown in Figs. 3 and 4. The formation of large grains resulted in small area of peripheral grain boundaries per unit area. We measured the total length of grain boundaries per unit area for the $Si_{0.8}Ge_{0.2}$ and $Si_{0.4}Ge_{0.6}$ films from the TEM
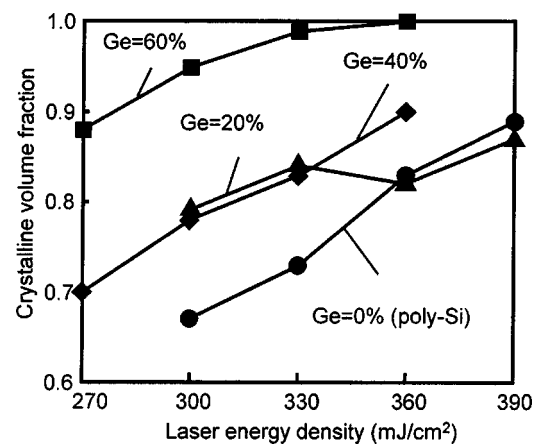

FIG. 5. Crystalline volume ratio, which was obtained by analysis of reflectivity spectra in ultraviolet region using a numerical calculation program, as a function of laser energy density for poly-SiGe films with different Ge concentrations.
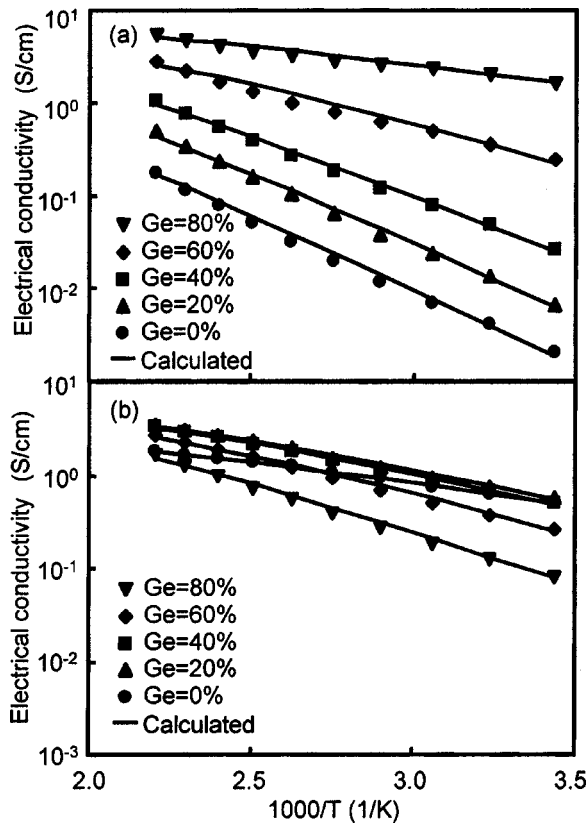
FIG. 6. Electrical conductivity as a reciprocal function of absolute temperature for poly-SiGe films with different Ge concentrations in as-crystallized (a) and with hydrogen plasma (b) cases. Hydrogen plasma treatment at 250 °C, 30 W, 130 Pa was carried out for 30 s. Solid marks show experimental electrical conductivities, and solid curves show calculated ones obtained by a numerical simulation program.
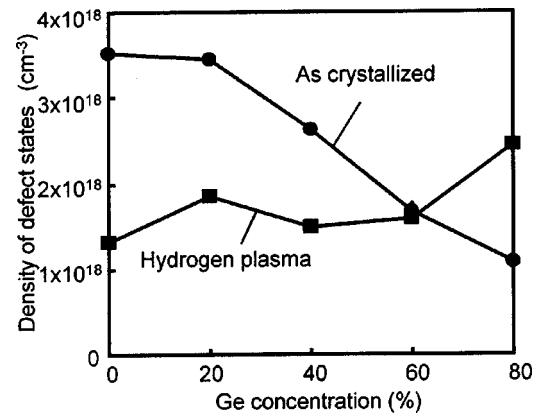

FIG. 7. Density of defect states, which were total density of tail-type and Gaussian-type defect states, obtained by the numerical calculation program, as a function of Ge concentration in as-crystallized and with hydrogen plasma treatment cases.

photographs given in Fig. 3. The total length of grain boundaries per unit area were 3.2×10^5 cm for $Si_{0.8}Ge_{0.2}$ films and 1.6×10^5 cm for $Si_{0.4}Ge_{0.6}$ films. 50% reduction of grain-boundary length was achieved from $Si_{0.8}Ge_{0.2}$ to $Si_{0.4}Ge_{0.6}$. From the results of crystalline volume ratio, the average width of electrical disordered states at grain boundaries (W_d) was estimated as

$$W_d = (1 - C) \times \frac{1}{L_d}, \qquad (3)$$

where C is the crystalline volume ratio obtained by E_2 peak analysis and L_d is the total length of grain boundaries per unit area. The width of electrical disordered states was estimated as 5.3 nm for $Si_{0.8}Ge_{0.2}$ films. Ten lattice layers had electrical disordered states at grain boundaries. In the case of $Si_{0.4}Ge_{0.6}$ film, the width of disordered states was less than 1.9 nm. It is interesting that laser crystallized SiGe films with a high Ge concentration of 60% had a narrow width of grain boundaries and a large grain size.

Figure 6 shows electrical conductivity as a reciprocal function of absolute temperature for poly-SiGe films as-crystallized (a) and with hydrogen plasma treatment (b). Solid marks show experimental electrical conductivities and solid curves show calculated ones obtained by a numerical simulation program. In the as-crystallized case, the electrical conductivity at room temperature increased from 2.0×10^{-3}

to 1.6 S/cm as Ge concentration increased from 0 to 80%, as shown in Fig. 6(a). The slope of electrical conductivity decreased as Ge concentration increased. Hydrogen plasma treatment effectively increased the electrical conductivity only for the Ge concentration from 0 to 40%, as shown in Fig. 6(b). Their slopes further decreased. However, hydrogen plasma treatment reduced the electrical conductivity for $Si_{0.2}Ge_{0.8}$ film.

In order to analyze the density of electrically active defects, a numerical calculation program was developed using finite element method with statistical thermodynamical conditions.[15,16] The potential energy for each element (φ_i) was calculated by Poisson equation, as shown by

$$\varphi_i = \varphi_{i+1} + \sum_{j=1}^{i} \frac{\rho_j}{\epsilon} d^2, \qquad (4)$$

where ρ_j is charge density for each element, ϵ is the dielectric constant of the poly-SiGe for each Ge concentration, and d is the distance of elements. Two types of defect states were introduced at grain boundaries. One is tail-type defect states, which have a peak density at conduction and valence band edges. The density was exponentially decreased toward to the midgap. The other is Gaussian-type defect states, which have a peak density at the midgap. The Fermi energy level was determined by the charge neutrality condition throughout the poly-SiGe films. Values of the effective density of states at the band edges, the specific dielectric constant, and the bandgap for each Ge concentration of single-crystalline SiGe were introduced into the calculation program. Fitting the calculated electrical conductivity to experimental one, as shown in Fig. 6, gave the density of defect states in the SiGe bandgap.

Figure 7 shows the density of defect states in the poly-SiGe films, which is the total density of tail-type and Gaussian-type defect states, estimated by the numerical calculation program as a function of Ge concentration for as-crystallized and with hydrogen plasma treatment cases. In the as-crystallized case, the density of defect states decreased from 3.5×10^{18} to 1.1×10^{18} cm^{-3} as Ge concentration increased from 0 to 80%. Those experimental results means

that laser-crystallized SiGe films with a high Ge concentration have low disordered defect states compared with laser-crystallized pure silicon films. From the results of the defect density and average grain size obtained by TEM observation, we calculated the density of defect states at grain boundary per unit area (D_g), as

$$D_g = D_p \times G, \tag{5}$$

where D_p is the density of defect states in the poly-SiGe films obtained by the numerical simulation program and G is the average grain size. The density of defect states at grain boundary were estimated to be 1.1×10^{13}, 1.0×10^{13}, and 6.8×10^{12} cm^{-2} for the $Si_{0.8}Ge_{0.2}$, $Si_{0.4}Ge_{0.6}$, and $Si_{0.2}Ge_{0.8}$ films, respectively. The density of defect states at the grain boundary gradually decreased as Ge concentration increased. The reduction in the defect density was probably associated with the reduction of the disordered region at grain boundary with increasing Ge concentration.

The density of defect states in the $Si_{0.8}Ge_{0.2}$ films was reduced from 3.5×10^{18} (as-crystallized) to 1.9×10^{18} cm^{-3} by hydrogen plasma treatment. The hydrogen plasma treatment effectively terminated dangling bonds in the films localized at grain boundaries, as we previously reported.[17,18] However, hydrogen plasma treatments did not reduce the defect density for $Si_{0.4}Ge_{0.6}$ and $Si_{0.2}Ge_{0.8}$ films. Although the physics is not clear, Ge–H bonding might be unstable at grain boundaries. Further experimental research is needed on defect passivation of poly-SiGe with the high Ge concentration as well as carrier scattering effects in order to achieve poly-SiGe with a low defect density and a high carrier mobility.

IV. SUMMARY

We investigated electrical and structural properties of poly-SiGe films fabricated using pulsed-laser annealing. Transient conductance measurement revealed that the maximum electrical conductivity of molten silicon increased from 210 to 4200 S/cm as Ge concentration increased from 0 to 80% at a laser energy density of 240 mJ/cm^2. It also increased from 1100 to 5100 S/cm at a laser energy density of 360 mJ/cm^2. On the other hand, the melt duration increased 30% as Ge concentration increased from 0 to 80%. The results mean that the solidification velocity increased as the Ge concentration increased. TEM measurement revealed that the average size of crystalline grains of poly-SiGe films increased from 66 to 120 nm as Ge concentration increased from 20% to 60%. This increase of the average crystalline grain size resulted from increase of crystallization velocity. The crystalline volume ratio, which was obtained by E_2 peak

analysis, also increased, from 0.83 to 1.0. The total length of grain boundaries per unit area was reduced from 3.2×10^5 to 1.6×10^5 cm as Ge concentration increased from 20% to 60%. The widths were consequently reduced from 5.3 to 1.9 nm. Analysis of an electrically active defect using a numerical calculation program revealed that the density of defect states decreased from 3.5×10^{18} to 1.1×10^{18} cm^{-3} as Ge concentration increased from 0 to 80%. This reduction was probably associated with the reduction of the disordered region, which was analyzed by TEM images and optical E_2 peak. In the case of $Si_{0.8}Ge_{0.2}$ films, 13.56-MHz hydrogen plasma treatment at 250 °C, 30 W, and 130 Pa for 30 s effectively reduced defect density from 3.5×10^{18} (as-crystallized) to 1.9×10^{18} cm^{-3}. However, the defect density was hardly changed by the plasma treatments for high-Ge-concentration samples.

[1] A. Kohno, T. Sameshima, N. Sano, M. Sekiya, and M. Hara, IEEE Trans. Electron Devices **ED-42**, 251 (1995).

[2] H. Watakabe and T. Sameshima, IEEE Trans. Electron Devices **ED-49**, 2217 (2002).

[3] H. Watakabe and T. Sameshima, Jpn. J. Appl. Phys. Part 2 **41**, L974 (2002).

[4] E. Fogarassy, B. Prevot, S. De Unamuno, M. Elliq, H. Pattyn, E. L. Mathe and A. Naudon, Appl. Phys. A **56**, 365 (1993).

[5] S. Higashi, D. Abe, Y. Hiroshima, and K. Miyashita, Jpn. J. Appl. Phys. **41**, 3646 (2002).

[6] T. Sameshima and S. Usui, J. Appl. Phys. **74**, 6592 (1993).

[7] I. Tsunoda, T. Nagata, A. Kenjo, T. Sadoh, and M. Miyao, Mater. Sci. Eng., B **89**, 336 (2002).

[8] T. Sameshima and S. Usui, Mater. Res. Soc. Symp. Proc. **258**, 117 (1992).

[9] C. Pickering and R. T. Carline, J. Appl. Phys. **75**, 4642 (1994).

[10] J. Humlicek, M. Garriga, M. I. Alonso, and M. Cardona, J. Appl. Phys. **65**, 2827 (1989).

[11] R. T. Carline, C. Pickering, D. J. Robbins, W. Y. Leong, A. D. Pitt, and A. G. Cullis, Appl. Phys. Lett. **64**, 1114 (1994).

[12] S. Yamaguchi, N. Sugii, K. Nakagawa, and M. Miyao, Jpn. J. Appl. Phys. **39**, 2054 (2000).

[13] S. R. Stiffler, M. O. Thompson, and P. S. Peercy, Phys. Rev. Lett. **60**, 2519 (1998).

[14] *Thermodynamic Properties of Individual Substances*, edited by L. V. Gurvich and I. V. Veyts (Hemisphere, New York, 1991), pp. 237 and 308.

[15] Y. Tsunoda, T. Sameshima, and S. Higashi, Jpn. J. Appl. Phys. **39**, 1656 (2000).

[16] K. Asada, K. Sakamoto, T. Watanabe, T. Sameshima, and S. Higashi, Jpn. J. Appl. Phys. **39**, 3883 (2000).

[17] T. Sameshima, M. Sekiya, M. Hara, and N. Sano, Jpn. J. Appl. Phys. **76**, 7377 (1994).

[18] K. Sakamoto, T. Sameshima, Y. Tsunoda, and S. Higashi, *Proc. of Workshop on Active Matrix Liquid Crystal Displays* Tokyo, Japan, 1999 (July 14–16, 1999, Kogakuin University, Copyright of Japan Society of Applied Physics), p. 131.